Supplementary Materials

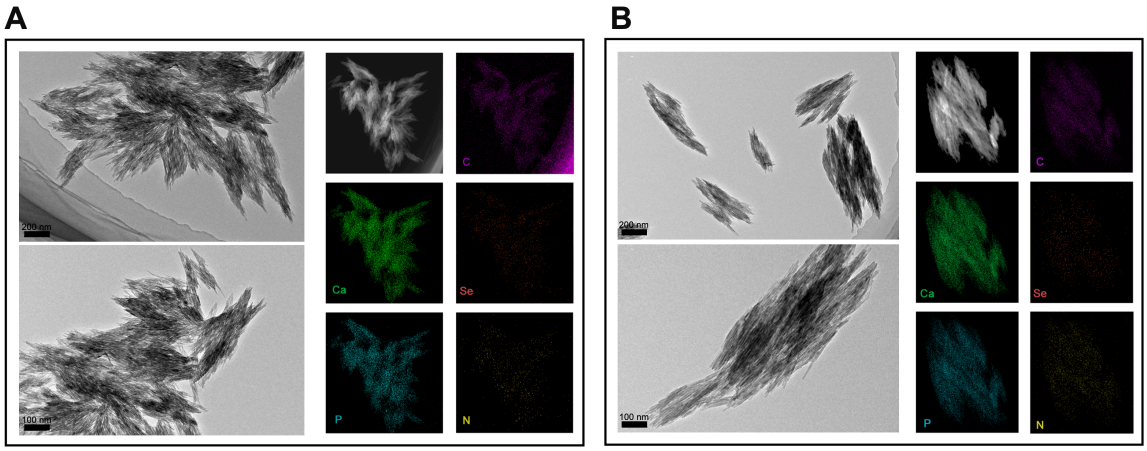

Fig. S1. TEM images and elemental mapping analysis of SeHANs and G3@SeHANs.

TEM images and elemental mapping analyses of (A) SeHANs and (B) G3@SeHANs. Elemental maps of carbon (C, purple), calcium (Ca, green), Se (red), phosphorus (P, blue), and nitrogen (N, yellow) are shown.

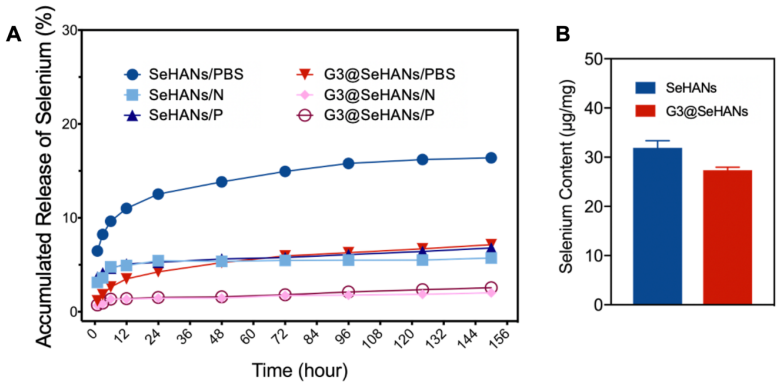

Fig. S2. Biodegradation and selenium release rate of SeHANs and G3@SeHANs.

The amount of selenium in synthesized nanoparticles was quantified using ICP-OES. (A) Selenium release by SeHANs and G3@SeHANs is indicative of their biodegradation and was detected by ICP-OES in three different solutions: PBS pH 7.4, saliva from healthy people (N), and saliva from periodontitis patients (P). (B) Selenium content of SeHANs and G3@SeHANs. Data are means ± SEM.

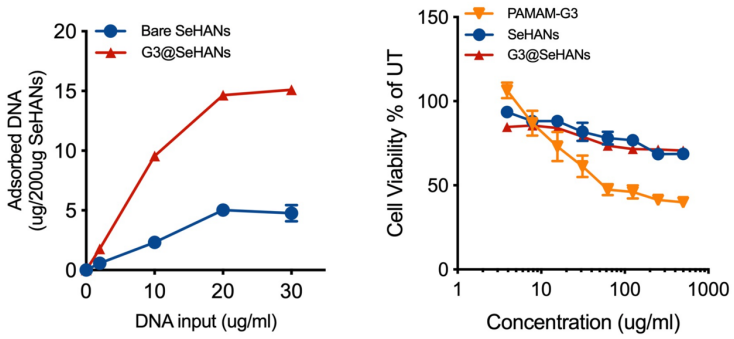

Fig. S3. DNA binding efficiency and cytotoxicity of SeHANs and G3@SeHANs.

(A) DNA binding efficiency of SeHANs and G3@SeHANs. (B) Viability of RAW 264.7 cells treated with PAMAM-G3, SeHANs, or G3@SeHANs at various concentrations for 24 h. Data means ± SEM.

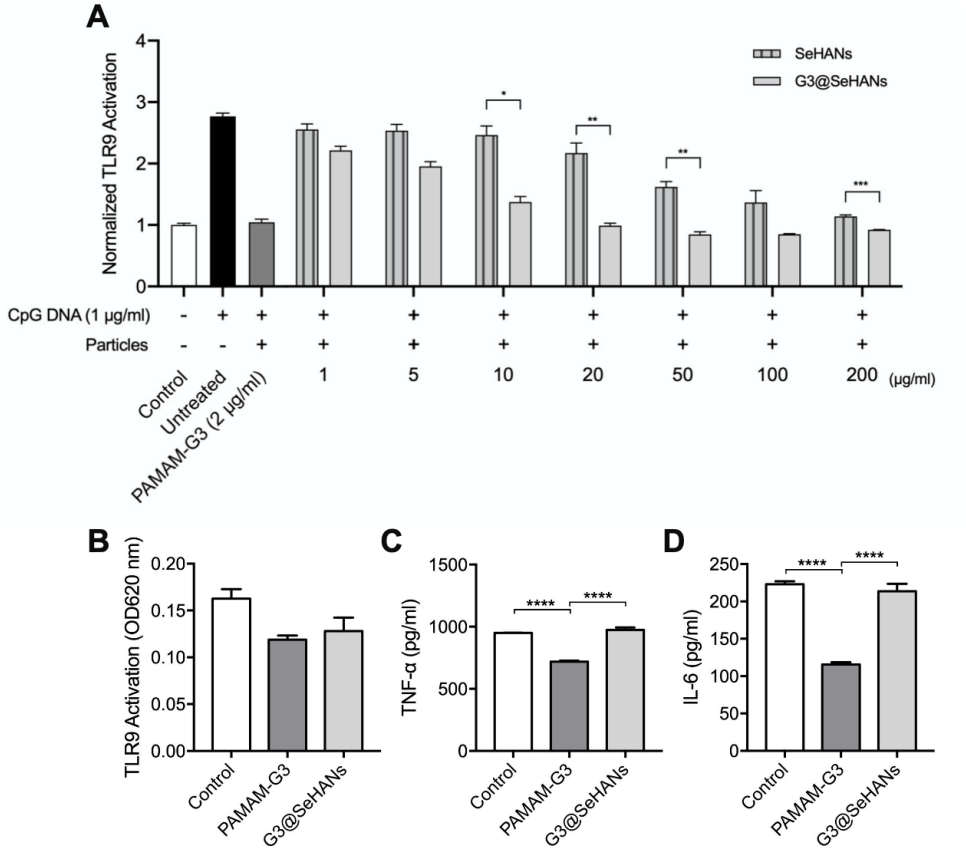

Fig. S4. Effects of bare SeHANs, G3@SeHANs, and PAMAM-G3 on cfDNA-induced proinflammatory response.

Activation of HEK-TLR9 reporter cells by (A) CpG DNA (1 μg/mL) in the absence or presence of SeHANs and G3@SeHANs at 1, 5, 10, 20, 50, 100, and 200 μg/mL for 24 h, and by (B) bare PAMAM-G3 (2 μg/mL) and G3@SeHANs (10 μg/mL) for 24 h. (C-D) TNF-α and IL-6 expression by RAW 264.7 macrophages treated with PAMAM-G3 (2 μg/mL) or G3@SeHANs (10 μg/mL) for 24 h. All data are means ± SEM; differences were assessed by one-way ANOVA with Tukey's multiple comparison test (n=3 independent experiments; *P<0.05, **P<0.01, ***P<0.001, ****P<0.0001).

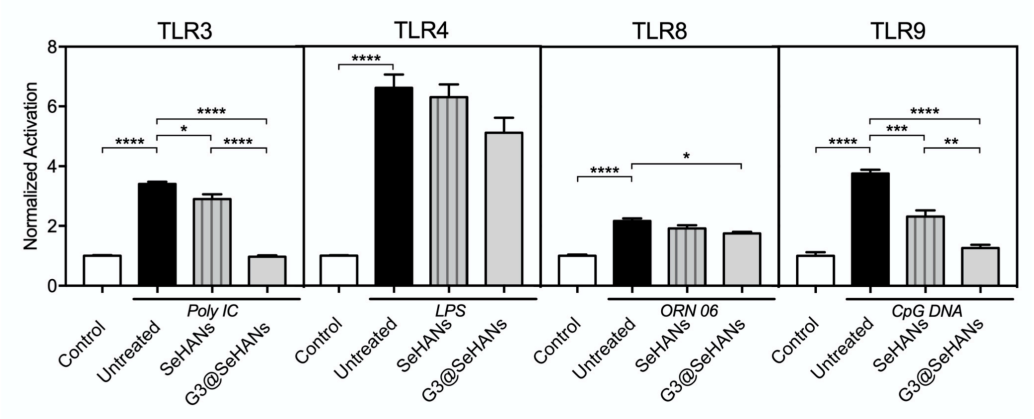

Fig. S5. G3@SeHANs limit the proinflammatory response *in vitro* through different TLR receptors.

Activation of HEK-TLR3, -TLR4, -TLR8, and -TLR9 reporter cells by poly(I:C) (1 μg/mL), LPS (1 ng/mL), ORN06 (500 ng/mL), and CpG DNA (1 μg/mL) in the absence or presence of PAMAM-G3 (2 μg/mL) or G3@SeHANs (10 μg/mL) for 24 h. Data are means ± SEM; differences were assessed by one-way ANOVA with Tukey's multiple comparison test; n=3 independent experiments; *P<0.05, **P<0.01, ***P<0.001, ****P<0.0001.

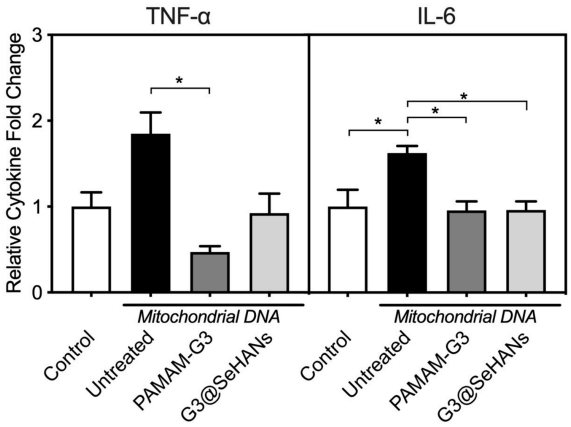

Fig. S6. NABNs block the mtDNA-driven proinflammatory response of THP-1 macrophages.

THP-1 macrophages were stimulated with mtDNA in the absence or presence of PAMAM-G3 (2 μg/mL) or G3@SeHANs (10 μg/mL) for 24 h. Supernatants were assayed for TNF-α and IL-6 by ELISA. Data are means ± SEM; differences were assessed by one-way ANOVA with Tukey's multiple comparison test; n=3 independent experiments; *P<0.05.

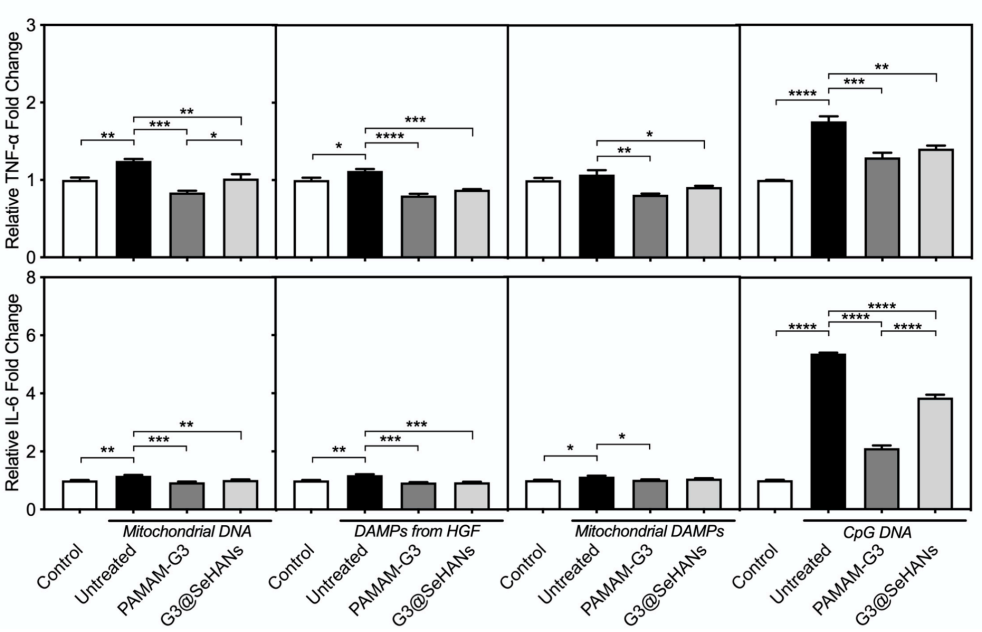

Fig. S7. NABNs block the proinflammatory response of DAMPs and DNA in RAW 264.7 macrophages.

RAW 264.7 macrophages were stimulated with mtDNA, DAMPs from gingival fibroblasts, DAMPs from mitochondria, or CpG DNA in the absence or presence of PAMAM-G3 (2 μg/mL) or G3@SeHANs (10 μg/mL) for 24 h. Supernatants were assayed for TNF-α and IL-6 by ELISA. Data are means ± SEM; differences were assessed by one-way ANOVA with Tukey's multiple comparison test; n=3 independent experiments; *P<0.05, **P<0.01, ***P<0.001, ****P<0.0001.

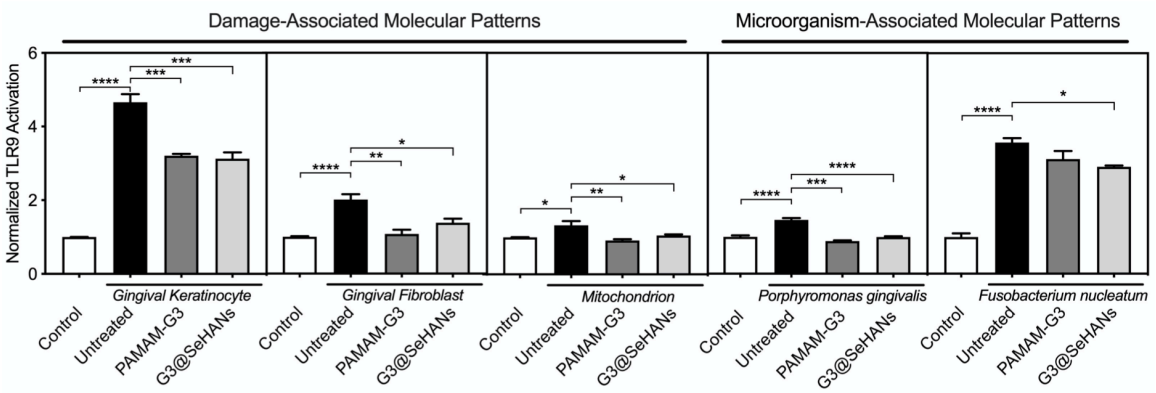

Fig. S8. NABNs block the DAMP- and MAMP-driven TLR9 proinflammatory response *in vitro*.

Activation of HEK-TLR9 reporter cells by DAMPs from gingival keratinocytes, gingival fibroblasts, mitochondria, and MAMPs from Pg, or Fn in the absence or presence of PAMAM-G3 (2 μg/mL) or G3@SeHANs (10 μg/mL) for 24 h. Data are means ± SEM; differences were assessed by one-way ANOVA with Tukey's multiple comparison test; n=3 independent experiments; *P<0.05, **P<0.01, ***P<0.001, ****P<0.0001.

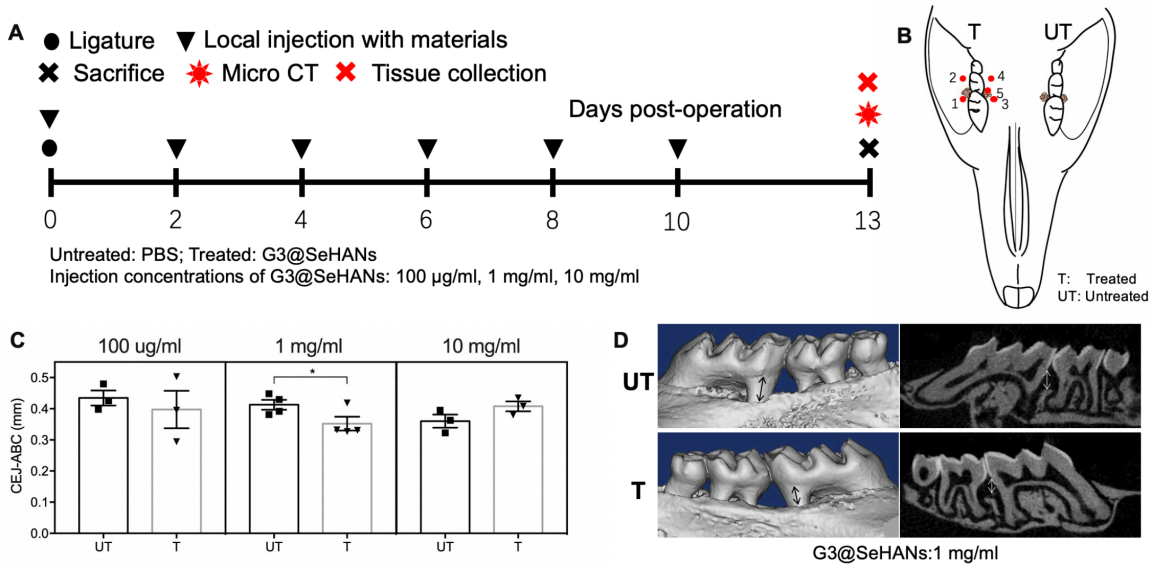

Fig. S9. Pilot animal study to determine NABN dose.

(A-B) Experimental schedule of the mouse study. The local administration of G3@SeHANs or PBS was performed by microinjection using a microsyringe into gingival tissue at five sites (5 μL/site) around the ligature every two days (on days 0, 2, 4, 6, 8, and 10) until the mice were sacrificed on day 13. For the pilot animal study, one side of the ligatures was treated with NABNs at three concentrations (100 μg/mL, 1 mg/mL, and 10 mg/mL) (treated, T), and the other side was injected with PBS (untreated, UT). (C) CEJ-ABC was used to measure bone loss. Different concentrations of NABNs were administered to determine the appropriate dose. Differences were assessed by Student's *t*-test. Data are means ± SEM; **P*<0.05. (D) 3D reconstruction and CT scans of the bone loss in the T and UT groups.

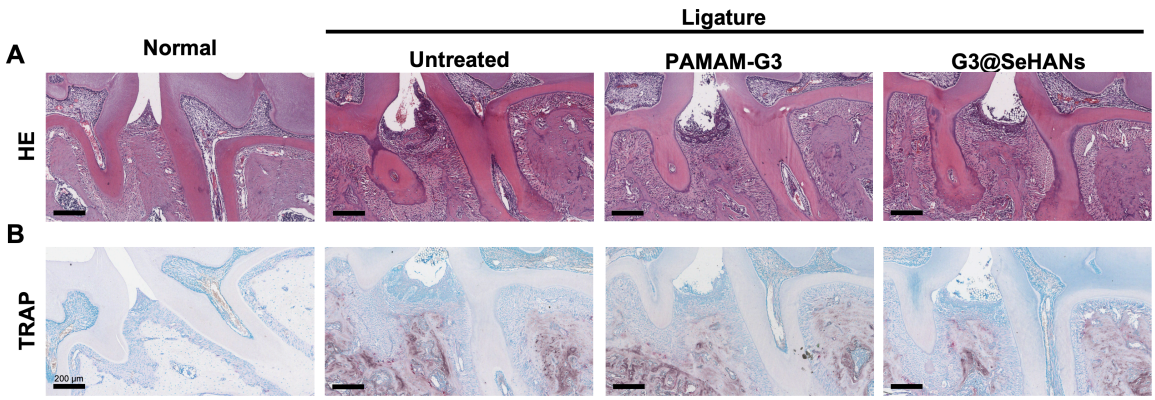

Fig. S10. H&E staining and TRAP/ALP staining of periodontal tissues at Day 15.

(A) H&E staining of periodontal tissues on day 15 after NABN administration (scale bars, 200 μm). Inflammatory cell infiltration in the epithelium and bone destruction were clearly evident in the untreated model, while treatment with NABNs efficiently prevented these pathological changes. (B) TRAP/ALP staining of periodontal tissues on day 15 after NABN administration (scale bars, 200 μm).

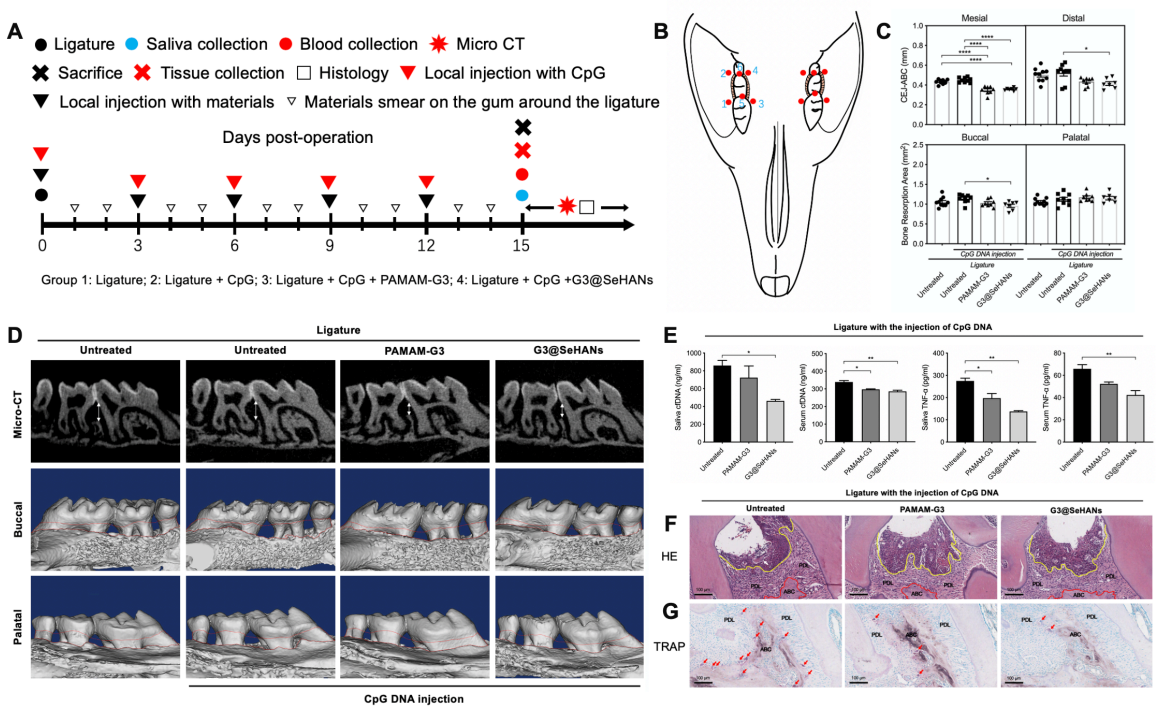

Fig. S11. cfDNA-enhanced inflammatory bone loss was alleviated by NABNs.

(A-B) Experimental schedule of the mouse study. The local injection of CpG was performed in addition to ligature placement. The injection of CpG was performed as described above 30 min after the injection of materials or PBS. (C) The CEJ-ABC was used to measure bone loss. The mesial and distal CEJ-ABC (μm) of the maxillary second molar was recorded. The bone resorption area was defined as the area enclosed by the continuous line of the CEJ of the three molars and the ABC. Data are means ± SEM; **P*<0.05, *****P*<0.0001 by one-way ANOVA with Tukey's multiple comparison test. (D) 3D reconstruction and CT scans of the bone loss in different groups. (E) Saliva cfDNA level, serum cfDNA level, saliva TNF-α level, and serum TNF-α level 15 days postoperation. Data are means ± SEM; *n*=3 samples per group, **P*<0.05, ***P*<0.01 by one-way ANOVA with Tukey's multiple comparison test. (F) H&E staining of periodontal tissues on day 15 (scale bars, 100 μm). (G) TRAP/ALP staining of periodontal tissues on day 15 (scale bars, 100 μm). The number of osteoclasts (red arrows) in the untreated group was higher than that in the scavenger-treated groups.

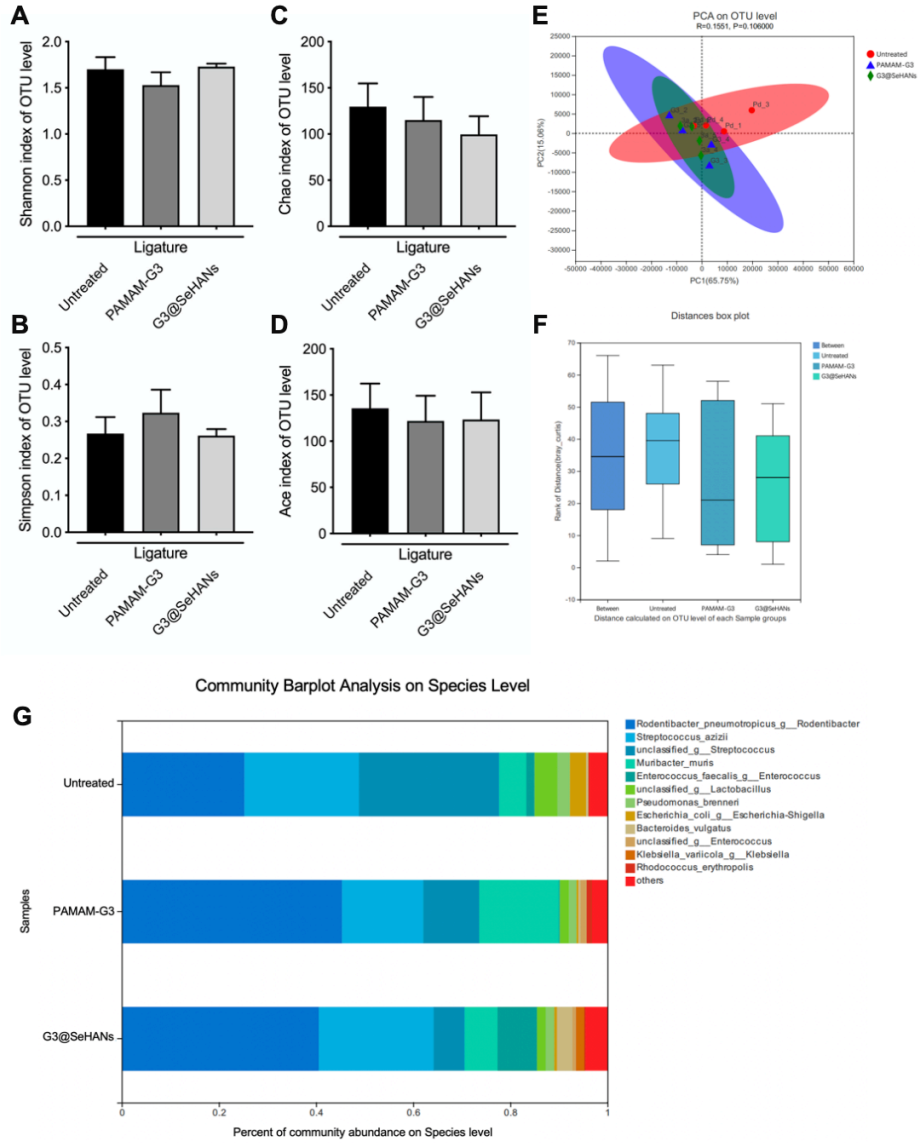

Fig. S12. Effects of NABNs on the oral microbiota of periodontitis mouse orally derived multispecies biofilms.

(A-D) Shannon index, Chao index, Simpson index, and Ace index at the OTU level. Data are means ± SEM; differences were assessed by one-way ANOVA with Tukey's multiple comparison test (n=4 samples per group). (E) PCA at the OTU level (n=4 samples per group). (F) Rank of the Bray-Curtis distance between or within groups (n=4). Statistical analyses were performed using ANOSIM. (D) Relative abundance of species-level taxa in the untreated, PAMAM-G3, and G3@SeHANs groups.

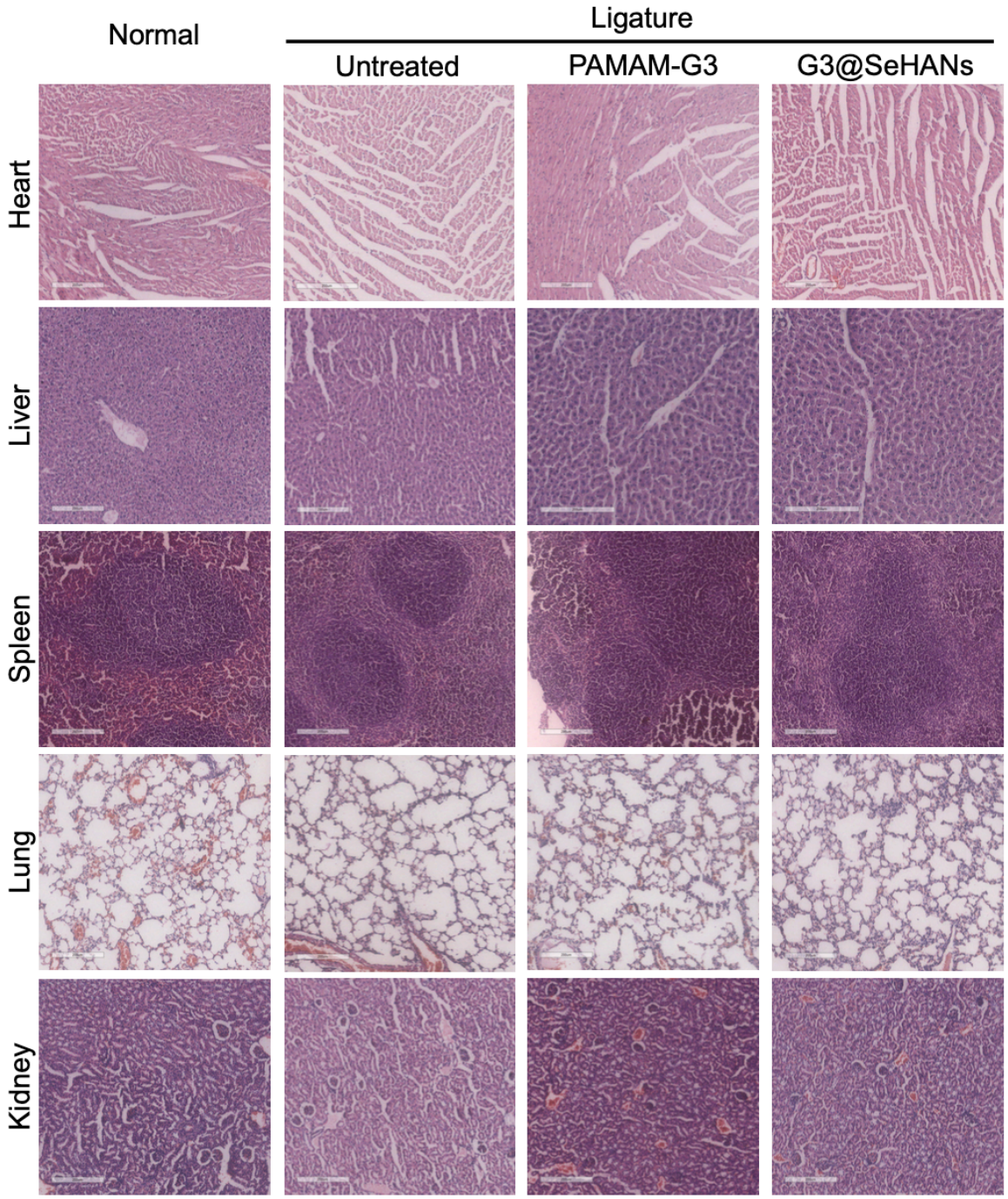

Fig. S13. H&E staining of multiple organs.

Fifteen days after the ligature was placed, the heart, liver, spleen, lung and kidney were collected, stained with H&E and analyzed. Scale bars, 200 μm. No obvious pathological change was found in the four groups.

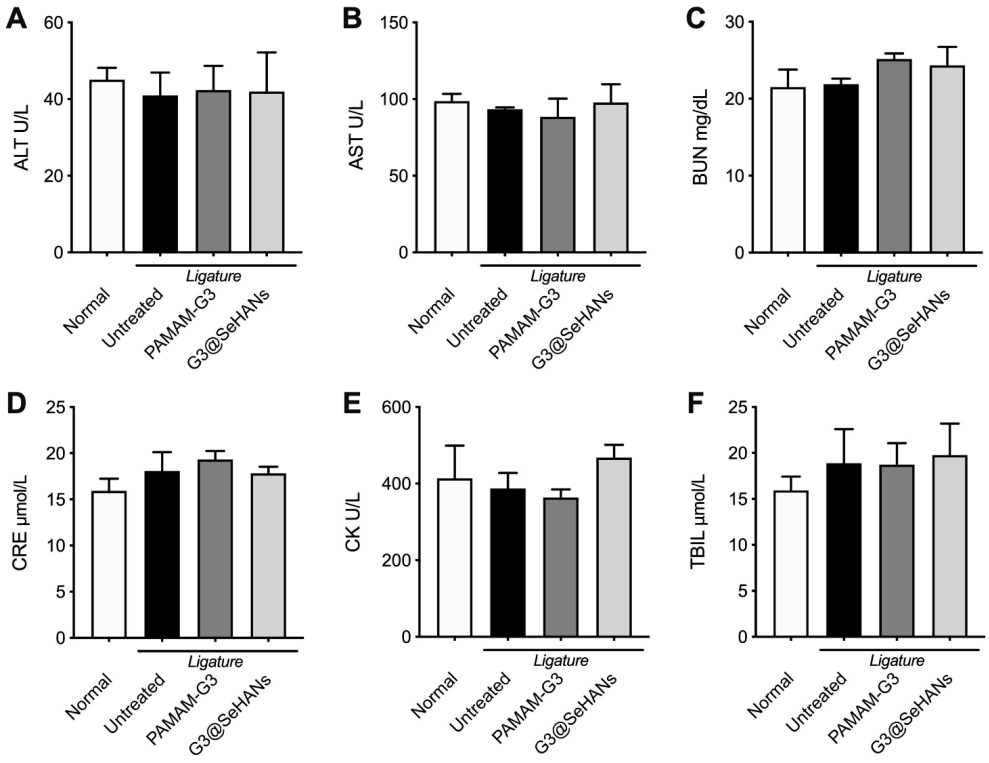

Fig. S14. Blood serum biochemistry parameters of mice.

The blood serum biochemistry parameters (A) ALT, (B) AST, (C) BUN, (D) CRE, (E) CK, and (F) TBIL of the four groups were measured. Differences were assessed by one-way ANOVA with Tukey's multiple comparison test (n=3 mice per group). Data are means ± SEM.

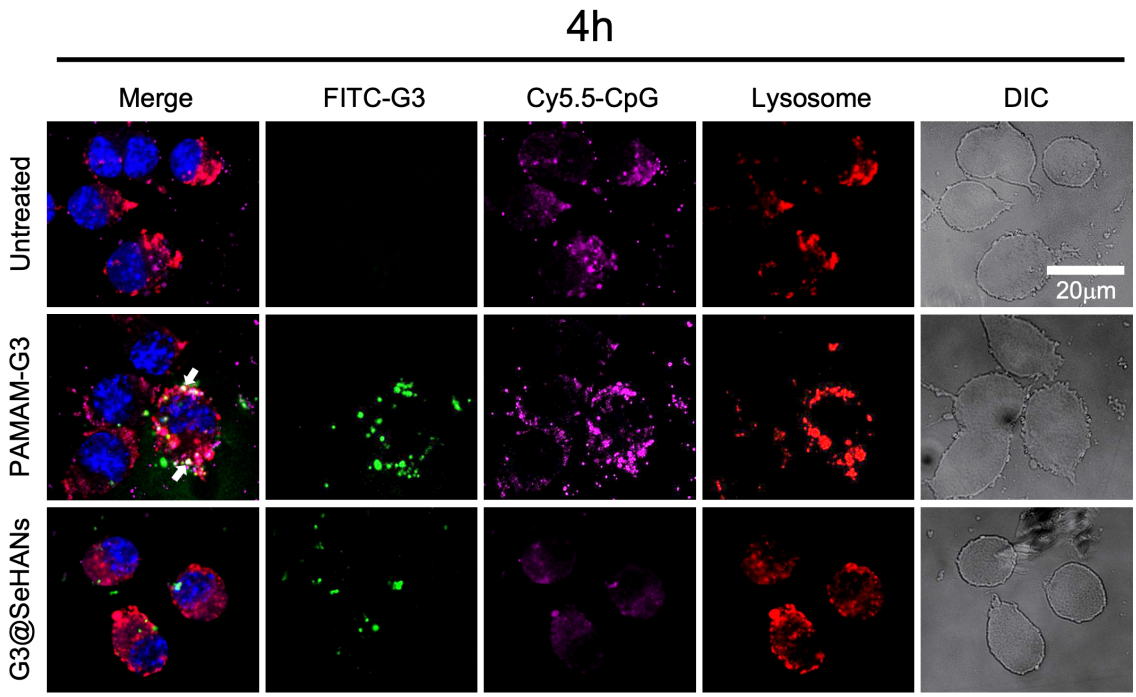

Fig. S15. Intracellular localization of intracellular CpG and cationic materials after a 4 h incubation.

Enlarged images showing the intracellular localization of intracellular CpG and cationic materials in RAW 264.7 cells after a 4 h incubation. The colocalization of CpG and cationic materials appeared as white spots, indicated by the arrows.

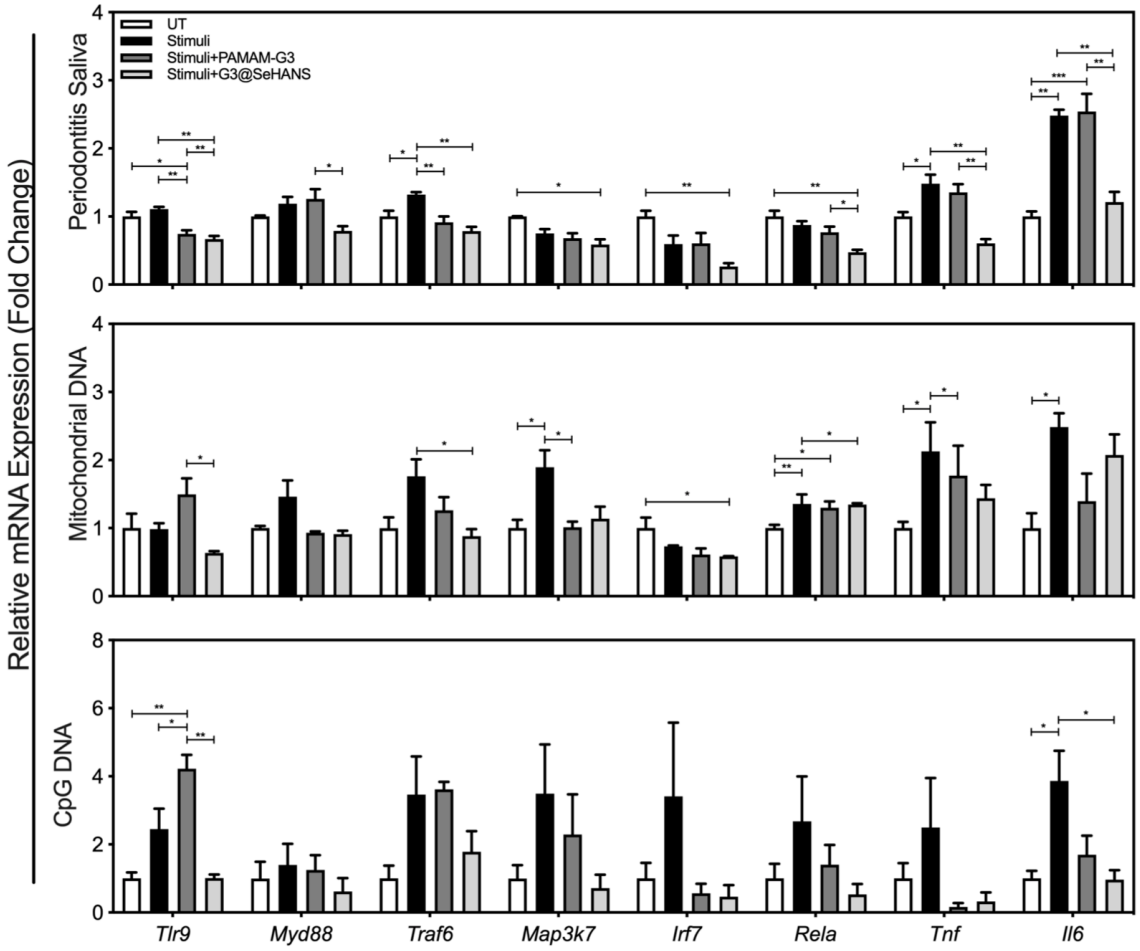

Fig. S16. Relative gene expression of the TLR9-NFκB pathway in RAW 264.7 cells with medium containing pathological DNA and scavengers.

Relative gene expression of the TLR9-NFκB pathway (*Tlr9*, *Myd88*, *Traf6*, *Map3k7*, *Irf7*, *Rela*, *Tnf*, and *Il6*) in RAW 264.7 cells after a 24 h incubation with medium containing pathological DNA and scavengers. The stimulus were added after 30 min of incubation with scavengers. Data are means ± SEM; n=3 samples per group; *P<0.05, **P<0.01, ***P<0.001 by one-way ANOVA with Tukey's multiple comparison test.

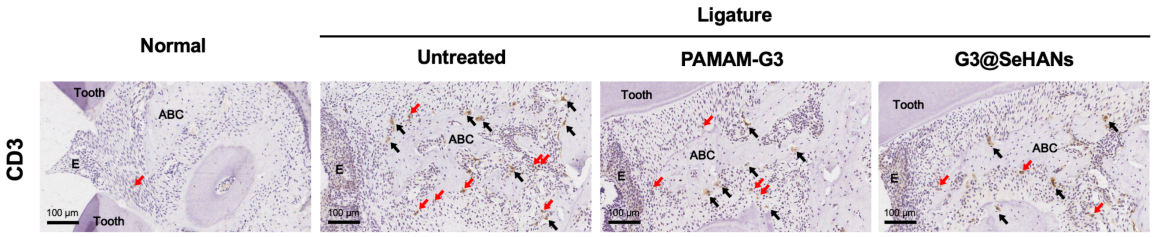

Fig. S17. IHC staining of T cells (CD3) in periodontal tissues on day 15.

IHC staining of T cells (CD3) in periodontal tissues on day 15 after NABN administration. Scale bars, 100 μm. CD3 IHC staining that the increased number of T cells in the untreated group could be controlled by scavenger treatment. Black arrows, osteoclasts; Red arrows, T cells; E, epithelium; ABC, alveolar bone crest.

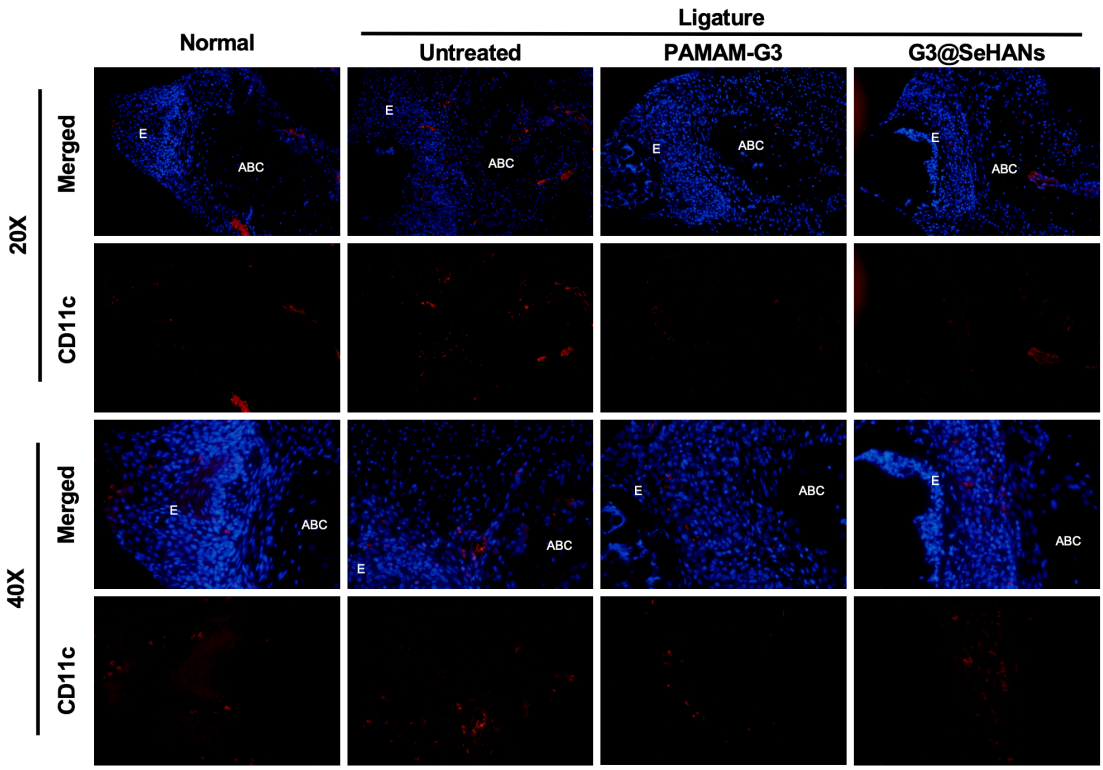

Fig. S18. IF staining of DCs (CD11c) in periodontal tissues on day 15.

CD11c IF staining (red) showed that the increased number of DCs in the untreated group could be controlled by scavenger treatment. E, epithelium; ABC, alveolar bone crest.

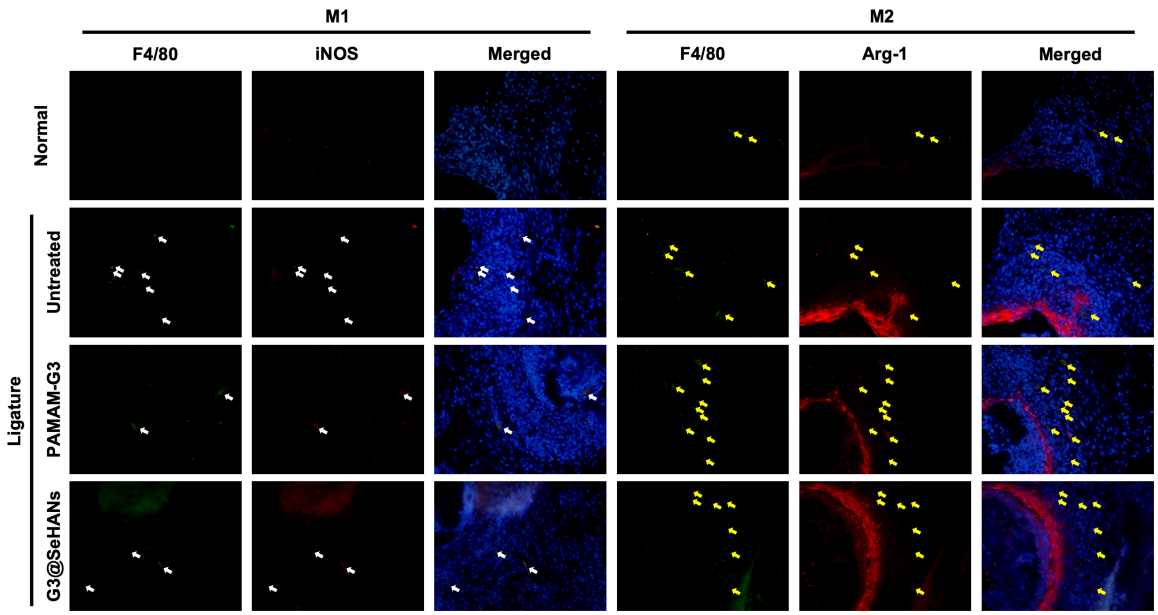

Fig. S19. IF staining showing polarization of macrophages in periodontal tissues on day 15.

Macrophages were detected with F4/80 (green). M1-type macrophages were marked with iNOS (red in the M1 column), and M2-type macrophages were marked with arginase-1 (red in the M2 column). DAPI was used to stain the cell nucleus (blue). Barely any M1 macrophages were found in the normal group, but the number of M1 macrophages was higher in the untreated group than the scavenger-treated groups. In contrast, the number of M2 macrophages increased in the scavenger-treated groups. Scale bars, 50 μm. White arrows, $F4/80^{+}iNOS^{+}$ cells (M1); yellow arrows, $F4/80^{+}Arg\text{-}1^{+}$ cells (M2).

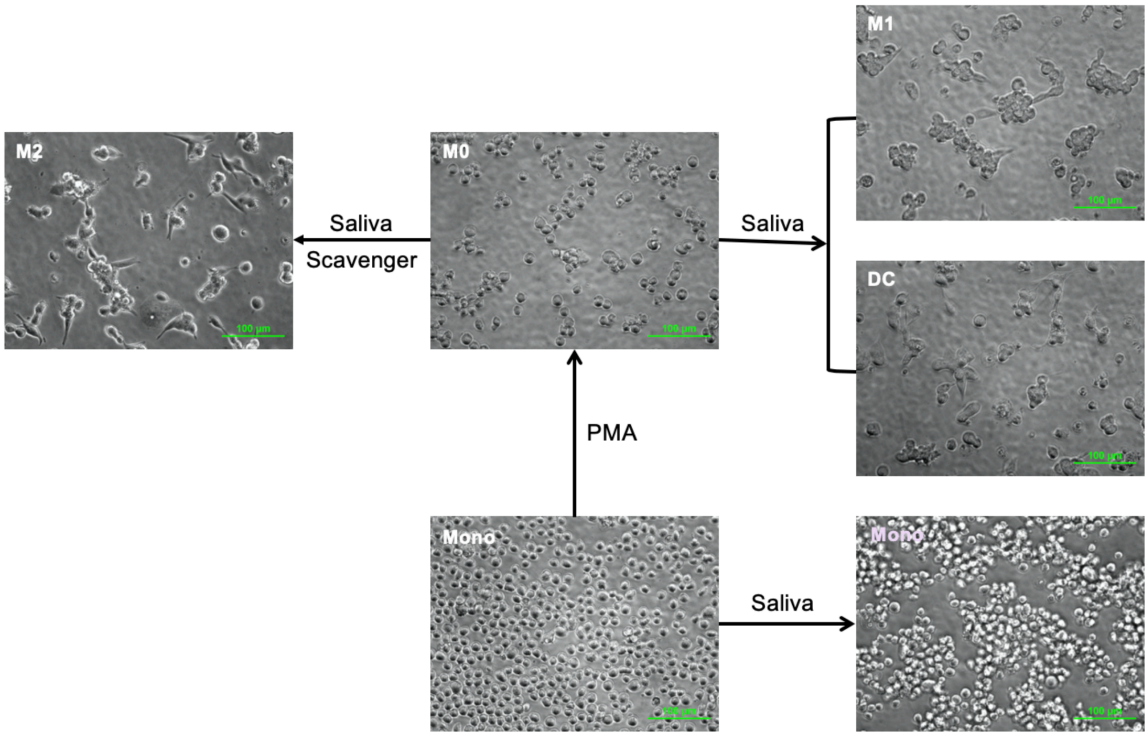

Fig. S20. Morphology of THP-1 cells treated with PMA, periodontitis saliva, and scavengers.

Mono, monocytes; M0, M0-phenotype macrophage; M1, M1-phenotype macrophage; M2, M2-phenotype macrophage; DC, dendritic cell. Scale bar, 100 μm.

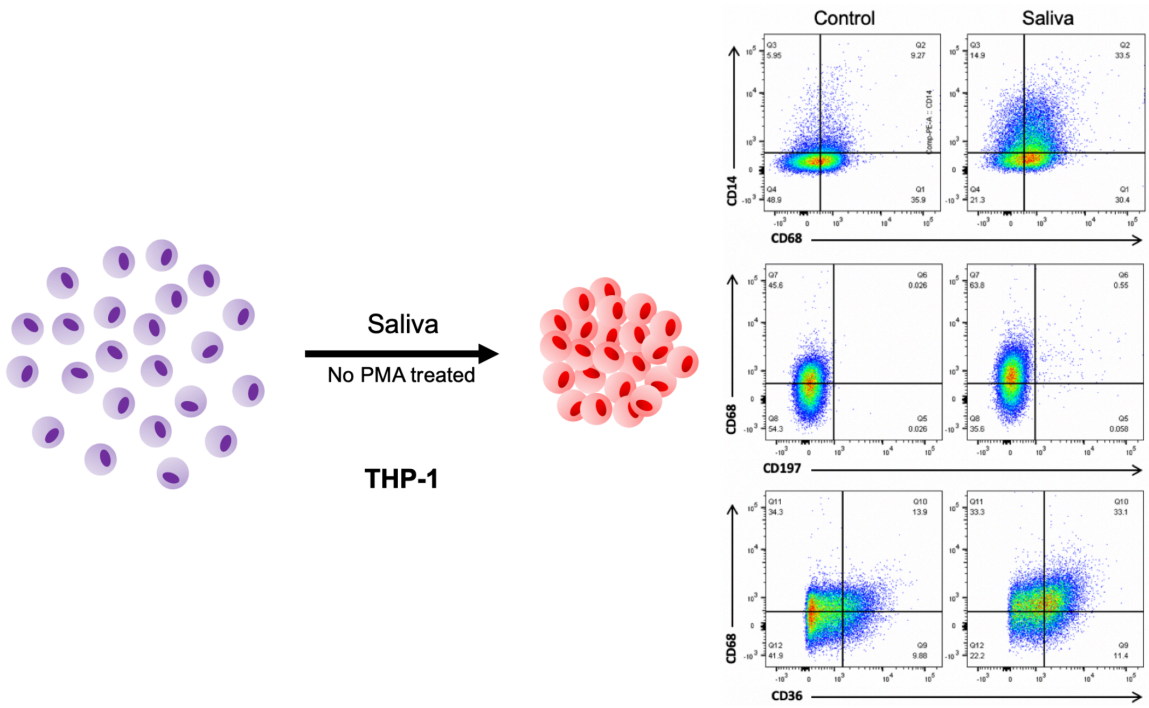

Fig. S21. THP-1 cells treated with periodontitis saliva without PMA.

THP-1 cells were agglomerated after incubation with periodontitis saliva. Flow cytometry of cell markers (CD14, CD68, CD197, and CD36) was performed.

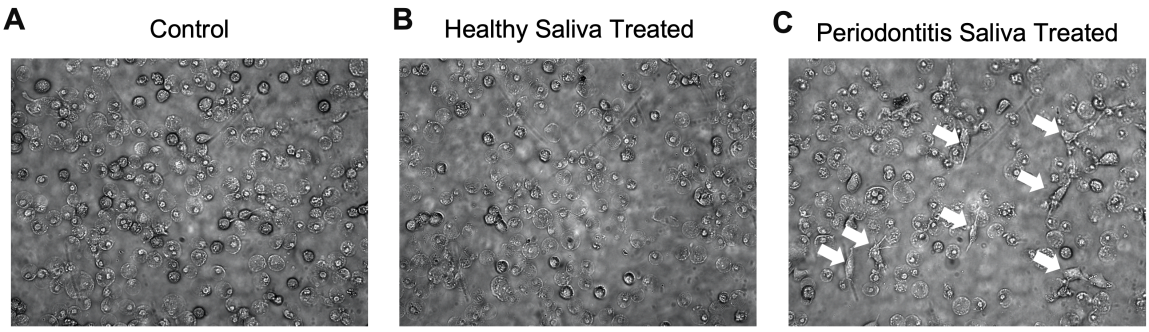

Fig. S22. Morphological changes of THP-1 cells incubated with healthy saliva and periodontitis saliva.

Morphology of THP-1 cells incubated with (A) only PMA, (B) PMA and healthy saliva, and (C) PMA and periodontitis saliva. Arrows show significant morphological changes in cells. Scale bar, 100 μm.

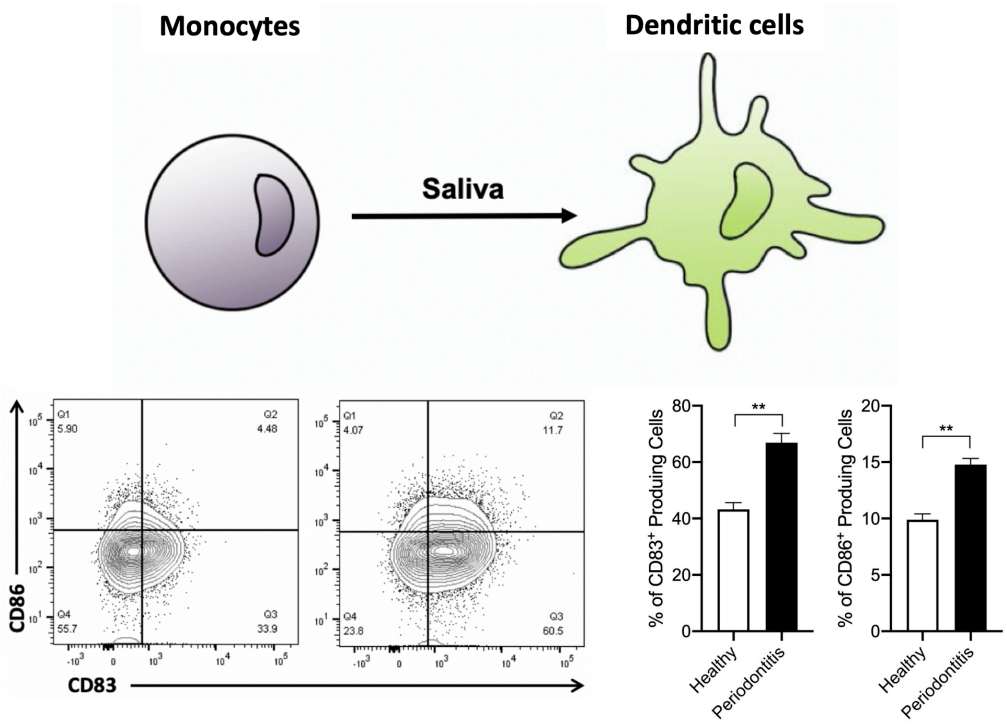

Fig. S23. DC differentiation of THP-1 cells treated with periodontitis saliva and PMA.

THP-1 cells showed the potential to differentiate into DCs after incubation with periodontitis saliva. Flow cytometry of cell markers (CD86 and CD83) was performed. Data are means ± SEM (n=3 samples per group; **P*<0.05, ***P*<0.01 by Student's *t* test).

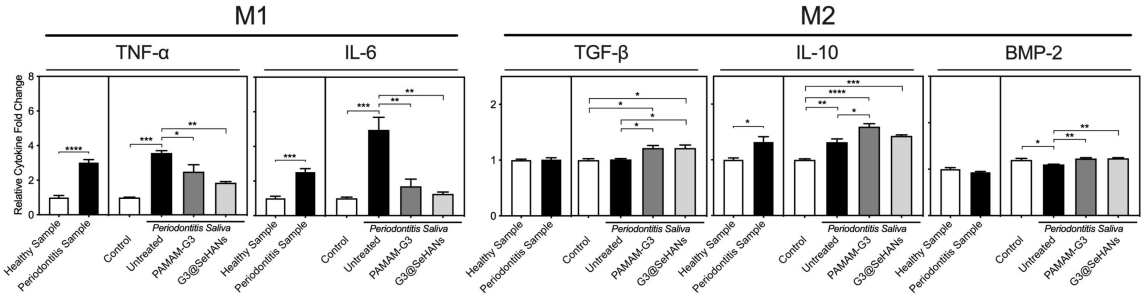

Fig. S24. Cytokine expression related to M1 and M2 macrophage phenotypes after incubation with periodontitis saliva and scavengers.

Activation of THP-1 cells by healthy human saliva or periodontitis patient saliva in the absence or presence of PAMAM-G3 (2 μg/mL) or G3@SeHANs (10 μg/mL). Supernatants were assayed for TNF-α, IL-6, TGF-β, IL-10, and BMP-2 by ELISA. Differences were assessed with a Student's *t*-test and one-way ANOVA with Tukey's multiple comparison test. Data are means ± SEM (n=3 independent experiments). *P<0.05, **P<0.01, ***P<0.001, ****P<0.0001.

Table S1. ANOSIM analysis of three groups at the OTU level.

Comparison between groups	R^2	*P* value
Untreated vs PAMAM-G3	0.1875	0.156
Untreated vs G3@SeHANs	0.1354	0.296
PAMAM-G3 vs G3@SeHANs	0.1146	0.336
Untreated vs PAMAM-G3 vs G3@SeHANs	0.1343	0.123

Table S2. Primers for qRT-PCR.

Primer	Forward	Reverse
Tlr9	TTCTCAAGACGGTGGATCGC	GCAGAGGGTTGCTTCTCACG
Myd88	CATGGTGGTGGTTGTTTCTGAC	TGGAGACAGGCTGAGTGCAA
Traf6	TGTTCTTAGCTGCTGGGGTGT	GAAGGAGCTGGAGAGGTTCC
Map3k7	ACAACATTGTAAAATGGCACAGGAG	TTTTGCTGGTCCTTTTCATCCT
Irf7	GAACTTAGCCGGGAGCTTGG	TGGAGCCCAGCATTTTCTCTT
Rela	TTCCTGGCGAGAGAAGCAC	AAGCTATGGATACTGCGGTCT
Tnf	AGGGTCTGGGCCATAGAACT	CCACCACGCTCTTCTGTCTAC
Il6	CTCTGCAAGAGACTTCCATCCAGT	GAAGTAGGGAAGGCCGTGG